

Umklapp-driven first-order transition into a charge-density wave phase

A.V. Rozhkov¹

¹*Institute for Theoretical and Applied Electrodynamics,
Russian Academy of Sciences, 125412 Moscow, Russia*
(Dated: May 30, 2025)

Using phenomenological Landau free energy, we systematically analyze influence of so-called umklapp contributions on the phase diagram of a solid hosting a commensurate charge-density wave phase. The umklapp terms may change the transition into the ordered state from continuous (second-order) to discontinuous (first-order). Additional elements, such as critical and tricritical points, emerge on the phase diagram under suitable conditions. The proposed mechanism is generalized for the case of nearly-commensurate charge-density wave, as well as spin-density wave orders. Several charge-density-wave-hosting alloys are used as experimentally available examples illustrating the formalism.

I. INTRODUCTION

Canonical theory of the charge-density wave (CDW) thermodynamic phase (e.g., Ref. 1) concludes that the transition from a disordered phase into a CDW state is continuous (second-order). This basic theoretical expectation is indeed confirmed by numerous experiments. For example, Fig. 5 in review paper 2 demonstrates continuous decay of the CDW order parameter to zero as a function of increasing temperature, for three different CDW-hosting alloys [NbSe₃, (TaSe₄)₂I, and K_{0.3}MoO₃]. As a more recently published instance of the same behavior, we can mention Fig. 3 in Ref. 3, where order-parameter-versus-temperature data for TiSe₂ are presented. Reference 4 examined the transition type for TbTe₃. Gradual decay of the order parameter, absence of hysteresis, and critical fluctuations all point to the continuous transition in the latter compound.

Yet for many crystals a CDW phase is separated from a disordered state by a discontinuous (first-order) transition. Namely, in IrTe₂ the formation of a commensurate CDW (CCDW) at temperature ~ 280 K is accompanied by pronounced hysteresis inside heating-cooling cycle^{5–9}, the signature of a first-order transition. Another alloy demonstrating the first-order transition between a CCDW and a disordered state is Lu₅Ir₄Si₁₀, with the CDW transition¹⁰ at 83 K.

In the interval between 130 K and 150 K a discontinuous transition into a nearly-commensurate CDW (NC-CDW) phase was reported¹¹ for Er₂Ir₃Si₅. Similarly, Lu₂Ir₃Si₅ enters NC-CDW phase through a first-order transition^{12–14}, with transition temperature ~ 200 K.

Various theoretical mechanisms^{15–22}, each with its own applicability range, are employed to explain the origins of discontinuous transition into a density-wave state. The most relevant for us here is a phenomenological approach pioneered in Ref. 16 to describe a CDW phase in TaSe₂.

The Landau-Ginzburg functional, specifically designed in the latter reference to account for peculiar features a CDW order, serves as a cornerstone of modern CDW modeling. Important concepts, such as “lock-in” NC-CDW-to-CCDW transition and order parameter “dislo-

cations”, were discussed. Investigation in Ref. 16 revealed that the so-called “umklapp” contributions to the Landau free energy can transform the continuous transition into a discontinuous one.

Here, we aim to explore systematically the influence of the umklapp terms, especially those of higher order, on the phase diagram of a CDW-hosting material. Constructing a suitable Landau free energy, we study phase transitions into commensurate and nearly-commensurate CDW states. We argue that in various rather general situations such transitions may become discontinuous. Moreover, for some conditions our theory predicts that a material can demonstrate two-transition sequence: a continuous normal-to-CCDW transition is followed by a first-order CCDW-CCDW transition, the latter connecting the states that differ only by order parameter magnitudes. (Note that a “lock-in” commensurate-incommensurate transition¹⁶ is a phenomenon of a distinctively dissimilar type, which will not be investigated below.)

As for NC-CDW, we show that, if non-CDW lattice distortions are incorporated into the model, suitably constructed umklapp terms become symmetry-allowed. When the lattice distortions fields are eliminated from the free energy, the resultant effective model is equivalent to CCDW Landau free energy, and a first-order transition can be recovered. We speculate that this scenario may explain a first-order transition within NC-CDW phase of EuTe₄ reported in Refs. 23–25.

Our paper is organized as follows. Section II is dedicated to formulation of a Landau free energy function valid for unidirectional incommensurate CDW. Various models of CCDW are introduced and analyzed in Sec. III. The case of NC-CDW is presented in Sec. IV. Our results are discussed in Sec. V. Technically involved calculations secondary to the main presentation are relegated to Appendices.

II. GENERAL CONSIDERATIONS

It is common to describe transition into a CDW state within the framework of the Landau free energy

$$F_0(\rho_{\text{cdw}}) = \frac{a}{2}|\rho_{\text{cdw}}|^2 + \frac{b}{4}|\rho_{\text{cdw}}|^4, \quad (1)$$

where the coefficients a and b satisfy the well-known conditions $b > 0$ and $a(T) = \alpha(T - T_{\text{CDW}})$. Here T is temperature, T_{CDW} is the CDW transition temperature, and coefficient α is positive.

As for the complex order parameter $\rho_{\text{cdw}} = |\rho_{\text{cdw}}|e^{i\varphi}$, it represents periodic charge-density modulation. In many situations it is conveniently approximated by a single harmonic term

$$\rho(\mathbf{R}) \approx \rho_{\text{cdw}}e^{i\mathbf{k}\cdot\mathbf{R}} + \text{c.c.} = 2|\rho_{\text{cdw}}|\cos(\mathbf{k}\cdot\mathbf{R} + \varphi), \quad (2)$$

where the wave vector \mathbf{k} characterizes CDW spatial periodicity. Following the standard prescription, one minimizes F_0 over ρ_{cdw} to derive

$$|\rho_{\text{cdw}}| = \theta(T_{\text{CDW}} - T) \sqrt{\frac{\alpha(T_{\text{CDW}} - T)}{b}}, \quad (3)$$

where $\theta(x)$ is the Heaviside step-function. This formula explicitly demonstrates that the order parameter strength $|\rho_{\text{cdw}}|$ is a continuous function of T , a hallmark of the second-order transition.

Unlike the absolute value $|\rho_{\text{cdw}}|$, the order parameter phase φ remains undetermined, which is a manifestation of the U(1)-symmetry of F_0 : the change

$$\varphi \rightarrow \varphi + \delta\varphi \quad (4)$$

keeps F_0 the same. Physically, this is a consequence of CDW free energy being invariant under arbitrary uniform translation

$$\mathbf{R} \rightarrow \mathbf{R} + \mathbf{t}, \quad \mathbf{t} \in \mathbb{R}^3. \quad (5)$$

It is easy to check that, for a given \mathbf{t} , the phase change is $\delta\varphi = (\mathbf{k}\cdot\mathbf{t})$, or, equivalently, the order parameter transforms according to

$$\rho_{\text{cdw}} \rightarrow \rho_{\text{cdw}}e^{i(\mathbf{k}\cdot\mathbf{t})} \quad (6)$$

under the translation \mathbf{t} .

III. COMMENSURATE CDW

A. Landau free energy with ‘umklapp’ contribution

The invariance of the CDW Landau free energy relative to arbitrary translations (5) is, by itself, a very excessive constraint on the model: in any crystal the translation group must be limited to lattice translations only, that is, instead of $\mathbf{t} \in \mathbb{R}^3$, the allowed \mathbf{t} ’s are

$$\mathbf{t} = m_1\mathbf{a}_1 + m_2\mathbf{a}_2 + m_3\mathbf{a}_3, \quad (7)$$

where m_i are integers, and \mathbf{a}_i are elementary lattice vectors.

The reduction of the invariance group implies that additional terms may be introduced into the Landau free energy. Below we explicitly construct these terms for commensurate CDW order.

By definition, a commensurate CDW satisfies the following conditions

$$(\mathbf{k}\cdot\mathbf{a}_i) = \frac{2\pi p_i}{q_i}, \quad i = 1, 2, 3, \quad (8)$$

where integer p_i is co-prime with q_i for all i . Formally, of course, any measured \mathbf{k} can be described in this manner, with arbitrary large q_i ’s. However, for practical matters, a wave vector is considered to be commensurate only when all three q_i ’s are not too large.

For these three q_i we introduce their least common multiple $n = \text{lcm}(q_1, q_2, q_3)$, referred below to as commensuration degree. Then the monomial ρ_{cdw}^n is invariant under arbitrary lattice translations. To prove this claim, we start with Eq. (6) and write $\rho_{\text{cdw}}^n \rightarrow \rho_{\text{cdw}}^n e^{i(\mathbf{k}\cdot\mathbf{t})n}$, where

$$(\mathbf{k}\cdot\mathbf{t})n = 2\pi \sum_i m_i p_i \frac{n}{q_i}. \quad (9)$$

Since n is a multiple of q_i for any i , one establishes that $(\mathbf{k}\cdot\mathbf{t})n = 2\pi N$, where N is an integer. Thus, ρ_{cdw}^n is invariant for any \mathbf{t} described by Eq. (7)

Note that, while n is formally introduced as the least common multiple of the three denominators, in many realistic situations, however, no significant number-theoretical calculations are required, as the commensuration degree is quite obvious from the data. For example, if $(p_1/q_1, p_2/q_2, p_3/q_3) = (1/5, 0, 1/5)$, as in Ref. 9, then $n = 5$.

Since ρ_{cdw}^n is invariant, we conclude that, for any complex number $c_n = |c_n|e^{i\gamma}$, the n th degree ‘umklapp’ contribution

$$F_u^{(n)} = -\frac{c_n}{2n}\rho_{\text{cdw}}^n + \text{c.c.} = -\frac{|c_n|}{n}|\rho_{\text{cdw}}|^n \cos(n\varphi + \gamma) \quad (10)$$

is explicitly real and invariant under lattice translations (similar expressions for the umklapp term, in a variety of settings, can be found^{15,26–28} in published literature).

Thus, the free energy

$$F^{(n)} = F_0 + F_u^{(n)} \quad (11)$$

can be used as a model for a commensurate CDW state. Note that inclusion of $F_u^{(n)}$ shrinks the symmetry group of the Landau energy from U(1) to Z_n : function $F^{(n)}$ is no longer invariant under an arbitrary phase shift, only discrete shifts

$$\varphi \rightarrow \varphi + \frac{2\pi m}{n}, \quad m \in \mathbb{Z}, \quad (12)$$

do not change the free energy.

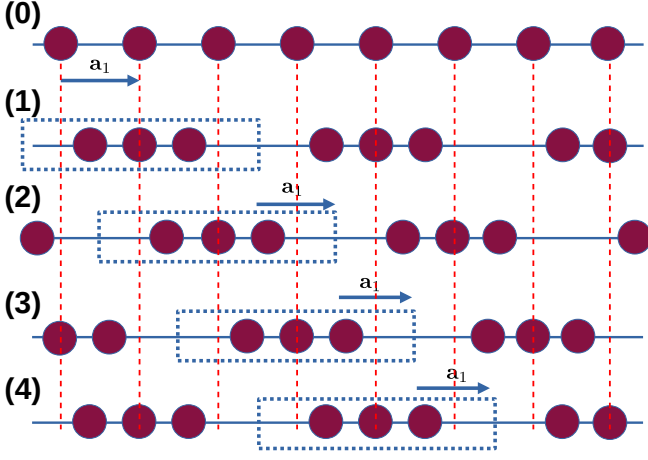


FIG. 1: Non-equivalent lattice configurations for a commensurate CDW for $n = 3$. Five panels schematically represent the same lattice with and without CCDW distortions. Primitive vector \mathbf{a}_1 of the unperturbed lattice (panel 0) is drawn as a (blue) arrow. The directions orthogonal to \mathbf{a}_1 are not depicted. Panels from 1 to 4 show the lattice distorted by the CDW. The CDW unit cell (dotted-line rectangle) grows three-fold relative to the unit cell of the pristine lattice. Vertical (red) dashed lines mark undistorted atoms positions. Starting from the CDW configuration in panel 1, one can generate two more structures (panels 2 and 3) by executing two consecutive translations on \mathbf{a}_1 . The third translation does not produce a new structure, instead the distortion shown in panel 1 is recovered, as indeed panel 4 demonstrates. Each configuration in panels 1, 2, and 3 represents one of three minima of the Z_3 model.

Let us now search for minima of $F^{(n)}$. Minimization with respect to φ is very simple. As this variable enters $F_u^{(n)}$ term only, it is easy to demonstrate that the Landau energy is the lowest when $\varphi = \varphi_m^*$, where

$$\varphi_m^* = \frac{2\pi m}{n} - \frac{\gamma}{n}, \quad m = 0, 1, \dots, n-1. \quad (13)$$

We see n minima evenly distributed over a unit circle. This arrangement resembles a clock dial, thus a common name for a model of this kind is the n -state clock model. Another frequently used designation is the Z_n model, a reference to the invariance group of $F^{(n)}$.

Every φ_m^* in Eq. (13) represents a particular localization of CDW distortions relative to the underlying lattice, see Fig. 1. There are n such localizations, all of them are degenerate. Speaking heuristically, one can say that a CDW with n th degree commensuration is always pinned by the lattice to one of n possible minima, as illustrated by Fig. 1. This pinning decreases the symmetry of the Landau free energy from $U(1)$ to Z_n .

At any of these minima the cosine in Eq. (10) is equal to unity. Thus, the Landau free energy can be re-written as a function of a single non-negative variable $|\rho_{\text{cdw}}|$

$$\tilde{F}^{(n)} = \frac{a}{2}|\rho_{\text{cdw}}|^2 + \frac{b}{4}|\rho_{\text{cdw}}|^4 - \frac{|c_n|}{n}|\rho_{\text{cdw}}|^n + \dots, \quad (14)$$

where ellipses stand for higher-order terms that might be required to maintain stability of the free energy. The tilde over F implies that this free energy does not depend on φ .

For $n = 2$ the contribution proportional to $|c_2|$ acts to renormalize a , effectively increasing the transition temperature. The transition remains continuous for all $|c_2|$. If $n > 2$, the contribution coming from the umklapp term $F_u^{(n)}$ may qualitatively alter the behavior of the system near the transition point, as discussed below.

B. Z_3 model of CDW

The value $n = 3$ represents the CCDW phase whose unit cell is three times larger than the unit cell of the underlying lattice. (This type of order is schematically shown in Fig. 1.) Specializing Eq. (14) for $n = 3$, one can express the free energy $\tilde{F}^{(3)}$ as

$$\tilde{F}^{(3)}(|\rho_{\text{cdw}}|) = \frac{a}{2}|\rho_{\text{cdw}}|^2 - \frac{|c_3|}{3}|\rho_{\text{cdw}}|^3 + \frac{b}{4}|\rho_{\text{cdw}}|^4. \quad (15)$$

We see that this free energy is stable in the sense that, for large $|\rho_{\text{cdw}}|$, function $\tilde{F}^{(3)}$ grows, which guarantees that an equilibrium value of the order parameter is bounded.

For $a > 0$ this free energy has a $|\rho_{\text{cdw}}| = 0$ minimum that represents (meta)stable disordered state. Additionally, for $a < |c_3|^2/(4b)$ there is a minimum of $\tilde{F}^{(3)}$ at

$$|\rho_{\text{cdw}}| = \frac{1}{2b} \left(|c_3| + \sqrt{|c_3|^2 - 4ab} \right), \quad (16)$$

see Fig. 2. It is easy to check that Eq. (16) describes the global minimum of $\tilde{F}^{(3)}$ when $a < 2|c_3|^2/(9b)$.

By exploiting the commonly assumed linearization

$$a = a(T) \approx \alpha(T - T_*), \quad \alpha > 0, \quad (17)$$

where T_* is the temperature for which $a(T)$ passes through zero, the CDW transition temperature can be expressed as

$$T_{\text{CDW}} = T_* + \frac{2|c_3|^2}{9\alpha b} > T_*. \quad (18)$$

We see that T_* by itself does not have any special meaning. However, in the limit $|c_3| \rightarrow 0$ the transition temperature T_{CDW} approaches T_* .

At the transition, the coefficient a is not zero, but rather $a = 2|c_3|^2/(9b)$. Substituting this value in Eq. (16), one finds that $|\rho_{\text{cdw}}|$ jumps from 0 to $2|c_3|/(3b)$, see also Fig. 2. Thus, we demonstrate that, at finite $|c_3|$, the transition is discontinuous. On the other hand, one must remember that at small $|c_3|$ the transition is formally indeed first-order, yet, in this regime, the discontinuity of order parameter becomes weak, and difficult to detect. This observation remains relevant for other signatures of first-order transition.

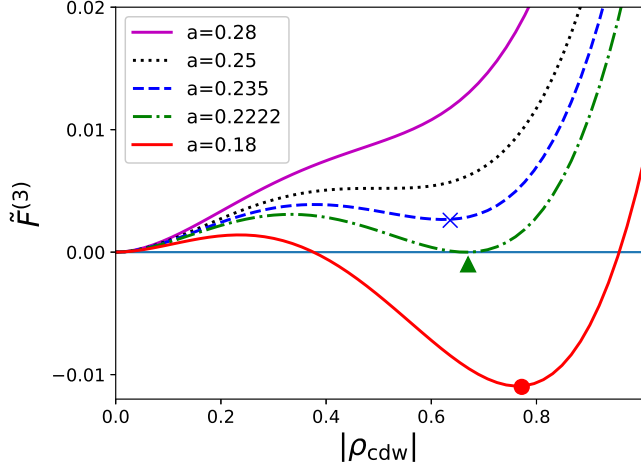


FIG. 2: Landau free energy $\tilde{F}^{(3)}$ as a function of the order parameter $|\rho_{\text{cdw}}|$, for various temperatures (various values of a , see legend). The graphs here are plotted for $b = 1$ and $|c_3| = 1$, all units are arbitrary. The solid (magenta) curve with a single minimum at $|\rho_{\text{cdw}}| = 0$ represents the system in the high-temperature disordered phase. The dashed (blue) curve with a non-trivial minimum (marked by the cross) shows the formation of the metastable CDW state at lower temperature (lower a). The dotted (black) curve separates the curves with and without a non-zero minimum. This separatrix is realized when $a(T) = |c_3|^2/(4b)$. If the trivial and non-trivial minima have identical free energies, which is the case of the dash-dotted (green) curve, the first-order phase transition occurs. Discontinuity of the order parameter at the transition is marked by (green) triangle. Solid (red) curve correspond to ordered phase, with the circle marking the stable value of $|\rho_{\text{cdw}}|$. The disordered phase $|\rho_{\text{cdw}}| = 0$ is a metastable minimum on this curve.

Concluding the discussion of the Z_3 -type models, we would like to note that, in the context of the CDW theory, cubic contributions to the Landau free energy are known for quite some time, at least since Ref. 16, where a CDW state in TaSe₂ was studied.

Note, however, that despite mathematical equivalence, the physical origins of the cubic term may differ, depending on specific details. In our derivation, we relied on condition (9) at $n = 3$ that demands of $3\mathbf{k}$ to be equal to a reciprocal lattice vector. Alternatively, when the three wave vectors of three co-existing CDW order parameters sum up to zero, a cubic term may emerge independently of requirement (9). Reference 16 discussed both of these mechanisms.

C. Z_4 model of CDW

The $n = 4$ phase diagram differs qualitatively from the $n = 3$ situation. The $n = 4$ Landau free energy reads

$$\tilde{F}^{(4)} = \frac{a}{2}|\rho_{\text{cdw}}|^2 + \frac{\tilde{b}}{4}|\rho_{\text{cdw}}|^4 + \frac{d}{6}|\rho_{\text{cdw}}|^6, \quad (19)$$

where $\tilde{b} = b - |c_4|$. In other words, $|c_4|$ effectively renormalizes b . Since \tilde{b} can be either positive, or negative, depending on the relation between b and $|c_4|$, we retained here the sixth-order term to prevent uncontrollable growth of the order parameter at $\tilde{b} < 0$.

When $|c_4| < b$, the free energy $\tilde{F}^{(4)}$ describes second-order transition that occurs at $a = 0$. If linearization (17) is assumed, then the transition temperature coincides with T_* .

At negative \tilde{b} , the transition into the CDW phase becomes first-order. (Qualitatively, the behavior of $\tilde{F}^{(4)}$ in this regime is very similar to the graphs of $\tilde{F}^{(3)}$ in Fig. 2.) For $0 < 4ad < \tilde{b}^2$ the free energy has three extrema: one at zero, and two more at

$$|\rho_{\text{cdw}}| = \sqrt{\frac{1}{2d} \left(|\tilde{b}| \pm \sqrt{\tilde{b}^2 - 4ad} \right)}. \quad (20)$$

The minimum (maximum) corresponds to the plus (minus) sign in this formula. The transition into the ordered state takes place when the free energy at the non-trivial minimum becomes zero, which is the free energy at the trivial minimum $|\rho_{\text{cdw}}| = 0$. This occurs at $a = 3\tilde{b}^2/(16d)$ if $\tilde{b} < 0$.

At arbitrary sign of \tilde{b} the transition temperature can be compactly expressed as

$$T_{\text{CDW}} = T_* + \frac{3(b - |c_4|)^2}{16ad} \theta(|c_4| - b). \quad (21)$$

This shows that, unlike the $n = 3$ case, arbitrary weak $n = 4$ umklapp term cannot change the continuous type of the transition. Only when $|c_4|$ exceeds b , the transition becomes discontinuous. The point $a = 0$, $|c_4| = b$ is a tricritical point on the phase diagram.

A version of the Z_4 theory was used by the authors of Refs. 29,30, who relied on a more complex Landau energy, with gradient terms, to investigate possible CDW lock-in transition. It appears, however, that their model was restricted by $\tilde{b} > 0$ condition. Under such a constraint a sixth-order term in the Landau free energy is not needed as the free energy remains stable for $\tilde{b} > 0$ even at fourth order. At the same time, one must remember that the tricritical point cannot be reached unless \tilde{b} is allowed to pass through zero.

D. Z_5 and Z_6 models

For $n = 5$ and $n = 6$, the phase diagram acquires additional complexity. We start our analysis by writing the $n = 5$ Landau free energy as

$$\tilde{F}^{(5)} = \frac{a}{2}|\rho_{\text{cdw}}|^2 + \frac{b}{4}|\rho_{\text{cdw}}|^4 - \frac{|c_5|}{5}|\rho_{\text{cdw}}|^5 + \frac{d}{6}|\rho_{\text{cdw}}|^6, \quad (22)$$

where, as before, we included the $O(|\rho_{\text{cdw}}|^6)$ term to provide proper growth of $\tilde{F}^{(5)}$ at $|\rho_{\text{cdw}}| \rightarrow +\infty$. Due to

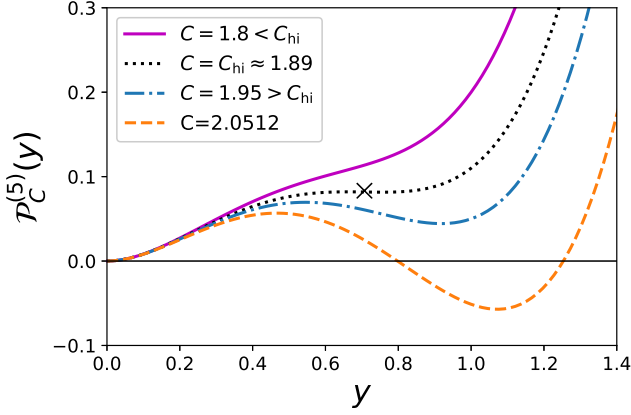


FIG. 3: Family of polynomials $\mathcal{P}_C^{(5)}(y)$, for various C , see legend. When $C < C_{\text{hi}} = 4\sqrt{2}/3$, the function increases monotonically for growing y (solid magenta curve), consequently, Eq. (26) has one non-zero root if $A < 0$, and no root otherwise. Exactly at $C = C_{\text{hi}}$ the polynomial graph (black dotted line) possesses a horizontal inflection point at $y = 1/\sqrt{2}$, which is marked by a cross. Below C_{hi} the function is no longer monotonic (dashed and dash-dotted curves). In this regime, for suitable A , multiple (two or three) roots of Eq. (26) exist. For sufficiently large values of C part of the curve lies below horizontal axis, as the (blue) dashed curve demonstrates. In this case, Eq. (26) has non-trivial roots even for positive A .

relative complexity of the $n = 5$ and $n = 6$ cases, it is convenient to introduce normalized quantities. Namely, the dimensionless form of $\tilde{F}^{(5)}$ reads

$$\frac{\tilde{F}^{(5)}}{\mathcal{F}_0} = \frac{A}{2}y^2 + \frac{1}{4}y^4 - \frac{C}{5}y^5 + \frac{1}{6}y^6. \quad (23)$$

The coefficient A in this formula is

$$A = \frac{ad}{b^2} = \frac{\alpha d}{b^2}(T - T_*). \quad (24)$$

Other quantities are

$$\mathcal{F}_0 = \frac{b^3}{d^2}, \quad y = \sqrt{\frac{d}{b}}|\rho_{\text{cdw}}|, \quad C = \frac{|c_5|}{\sqrt{bd}}. \quad (25)$$

Here energy \mathcal{F}_0 sets the overall scale for $\tilde{F}^{(5)}$, and y is the dimensionless order parameter.

For $A < 0$, the disordered state $y = 0$ is absolutely unstable. It is at least metastable when $A > 0$. As for ordered states (stable, metastable, or unstable), they are represented by roots of the equation

$$\mathcal{P}_C^{(5)}(y) = -A, \quad (26)$$

where $\mathcal{P}_C^{(5)}(y)$ is a family of polynomials of variable y

$$\mathcal{P}_C^{(5)}(y) = y^2(1 - Cy + y^2), \quad (27)$$

parameterized by $C > 0$.

For small C and positive y , the polynomials are positive increasing functions, see Fig. 3. Thus, Eq. (26) has one solution for negative A . No solution exists when $A > 0$. If C is fixed, this describes an order-disorder continuous phase transition at $A = 0$, or, equivalently, at $T = T_*$.

This simple picture is not applicable for $C > C_{\text{hi}} = 4\sqrt{2}/3$. Indeed, at $C = C_{\text{hi}}$ a horizontal inflection at $y = 1/\sqrt{2}$ is formed (hence, the subscript ‘hi’). For $C > C_{\text{hi}}$ the polynomial $\mathcal{P}_C^{(5)}(y)$ is no longer monotonic as a function of y , and more than one solution become possible for appropriate (negative) values of A . Since $\mathcal{P}_{C_{\text{hi}}}(1/\sqrt{2}) = 1/12$, multiple roots are realized for $A > -1/12$. Multiple non-trivial roots of Eq. (26) implies that a first-order transition between CDW states emerges. Note that the states separated by this transition have identical symmetries. The only difference between these states is the magnitude of $|\rho_{\text{cdw}}|$, which abruptly changes upon crossing the transition line.

As one can see from Fig. 3, for sufficiently large C there are finite intervals of y in which the value $\mathcal{P}_C^{(5)}(y)$ is negative. For such C , Eq. (26) has two roots even for positive A . When A grows, the roots approach each other, merge, and ultimately disappear, signaling disappearance of a (meta)stable CDW minimum.

The resultant phase diagram is shown in Fig. 4 (left). It features a second-order transition line reaching the first-order transition curve. The latter terminates at a critical point inside the CDW phase. This point corresponds to the horizontal inflection point for $\mathcal{P}_C^{(5)}$. The location of the tricritical point ‘T’, where two transition lines meet, is characterized by the presence, at $A = 0$, of a non-zero root of Eq. (26) that additionally satisfies $\tilde{F}^{(5)}(y) = 0$. These requirements are fulfilled when $C = 5/\sqrt{6}$, which is the horizontal coordinate of ‘T’.

Depending on the value of C , the behavior $\rho_{\text{cdw}} = \rho_{\text{cdw}}(T)$ may vary significantly, see Fig. 5. If $C > 5/\sqrt{6}$, which corresponds to the area to the right of the ‘T’ on the phase diagram, the order-disorder transition is discontinuous. To the left of point ‘Cp’ ($C < 4\sqrt{2}/3$), the transition is continuous, at $A = 0$. In the interval $4\sqrt{2}/3 < C < 5/\sqrt{6}$ the model exhibits a cascade of two transitions (a first-order CDW-CDW transition followed by a second-order CDW-disorder transition). When coefficient C is fine-tuned to be $C = 4\sqrt{2}/3$, the order parameter discontinuity shrinks to zero and becomes a continuous singularity, as shown in Fig. 5.

For $n = 6$ commensuration, the Landau free energy can be expressed as

$$\tilde{F}^{(6)} = \frac{a}{2}|\rho_{\text{cdw}}|^2 + \frac{b}{4}|\rho_{\text{cdw}}|^4 - \frac{\tilde{d}}{6}|\rho_{\text{cdw}}|^6 + \frac{e}{8}|\rho_{\text{cdw}}|^8, \quad (28)$$

where $\tilde{d} = |c_6| - d$, and $d, e > 0$. Normalized form of this free energy is easy to establish

$$\frac{\tilde{F}^{(6)}}{\mathcal{F}_0} = \frac{A}{2}y^2 + \frac{1}{4}y^4 - \frac{D}{6}y^6 + \frac{1}{8}y^8. \quad (29)$$

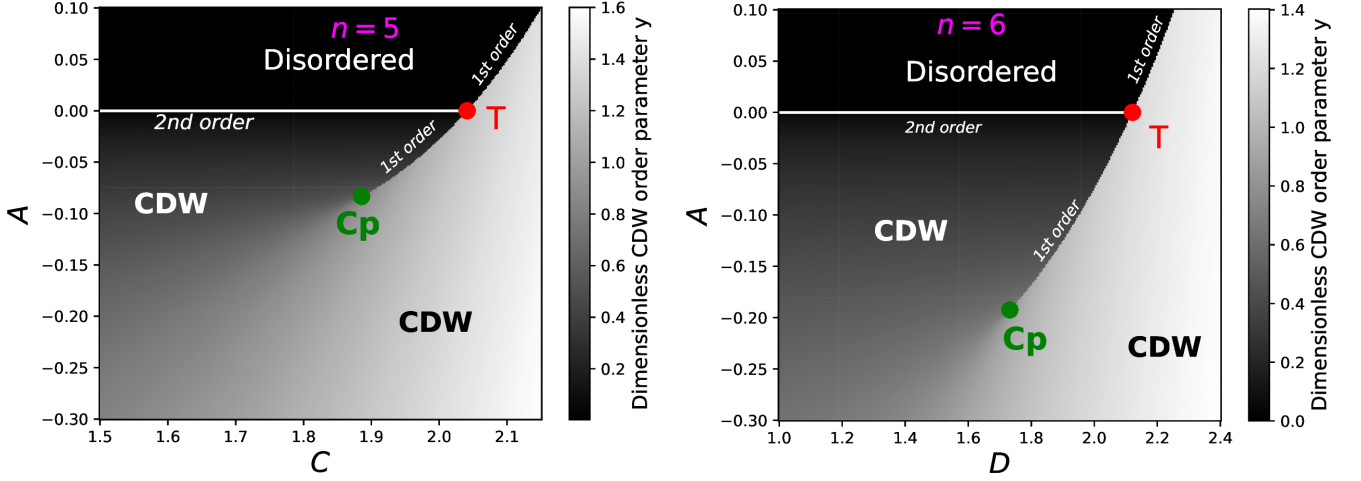


FIG. 4: Grayscale phase diagrams for $n = 5$ (left) and $n = 6$ (right). The diagrams are results of numerical minimization of the dimensionless Landau free energies $\tilde{F}^{(5,6)}/\mathcal{F}_0$, see Eqs. (23) and (29), over dimensionless order parameter y . Black area represents the disordered phase, various shades of gray express the CDW order parameter strength (for references, see a colorbar to the right of a respective phase diagram). The disordered phase is bound on the right by a first-order transition line visible as a sharp contrast edge. This first-order line intrudes into the CDW phase terminating in a critical point (green dot marked by ‘Cp’). Inside the ordered phase this line separates the CDW states with unequal value of y (crossing this line from left to right we see discontinuous growth of y). The critical point ‘Cp’ corresponds to polynomial $\mathcal{P}_{C,D}^{(5,6)}$ with the horizontal inflection point [for $n = 5$ ($n = 6$) this inflection occurs at $C = 4\sqrt{2}/3 \approx 1.89$ (at $D = \sqrt{3} \approx 1.73$)]. The second-order transition line at $A = 0$ limits the disordered phase from below. For $n = 5$ this line reaches the first-order transition curve at $C = 5/\sqrt{6} \approx 2.04$ and terminates there (this tricritical point is marked by a red dot and ‘T’). When $n = 6$, point ‘T’ is located at $D = 3/\sqrt{2} \approx 2.12$. Qualitative structures of the two phase diagrams are identical.

Here, under assumption $b > 0$, we introduced the following set of parameters

$$y = \left(\frac{e}{b}\right)^{1/4} |\rho_{\text{cdw}}|, \quad \mathcal{F}_0 = \frac{b^2}{e}, \quad (30)$$

$$A = a\sqrt{\frac{e}{b^3}}, \quad D = \frac{\tilde{d}}{\sqrt{be}}. \quad (31)$$

Similar to Eq. (26), ordered phases of the $n = 6$ model are represented by roots of equation

$$\mathcal{P}_D^{(6)}(y) = -A, \quad \text{where} \quad \mathcal{P}_D^{(6)} = y^2(1 - Dy^2 + y^4). \quad (32)$$

Analysis of Eq. (26) can be adopted for the latter equation, and an $n = 6$ phase diagram can be constructed, see Fig. 4 (right). It is clear that both diagrams in Fig. 4 are qualitatively similar.

The Z_5 model can be used to describe the first-order transition in IrTe_2 . Specifically, at $T \sim 280$ K the compound enters³¹ a CDW phase with $\mathbf{k} = (1/5, 0, 1/5)$. Obviously, this phase fits the Z_5 case. Observed hysteresis and resistivity discontinuities indicate a first-order transition. Since no incommensurate order was reported, the lock-in scenario can be excluded. This implies relevance of the phase diagram in Fig. 4 (left).

At lower temperature the $n = 5$ phase in IrTe_2 is replaced by a $n = 8$ CDW state. The transitions are sensitive to pressure and Ir-to-Pt chemical substitution. Thus, one can consider constructing a more comprehensive phase diagram that accounts for these circumstances.

Such a deserving task, however, must be deferred to future research.

As for the Z_6 model, it will be of use for the discussion of EuTe_4 , see next section.

IV. NEAR-COMMENSURATE CDW

We demonstrated in the previous section that symmetry-allowed umklapp terms enhance complexity of the model’s phase diagram. In particular, a first-order transition line emerges. Let us now generalize our approach to the case of NC-CDW.

For an NC-CDW, vector $n\mathbf{k}$ does not belong to the reciprocal lattice of a host crystal for any $n \in \mathbb{N}$, however, one can find a (small) integer m and a reciprocal lattice vector $\mathbf{b} \neq 0$ such that a “defect” vector

$$\mathbf{p} = \mathbf{b} - m\mathbf{k} \quad (33)$$

is small in the sense that $|(\mathbf{p} \cdot \mathbf{a}_i)| \ll 1$ for all $i = 1, 2, 3$.

Since \mathbf{k} is not commensurate, ρ_{cdw}^n is not compatible with the lattice translation group for any $n \in \mathbb{N}$. Yet, an umklapp contribution associated with the NC-CDW order can emerge through the following mechanism. Note that a monomial ρ_{cdw}^m , where m is defined in Eq. (33), transforms according to the rule $\rho_{\text{cdw}}^m \rightarrow e^{-i(\mathbf{p} \cdot \mathbf{a}_i)} \rho_{\text{cdw}}^m$ upon a translation on the elementary lattice vector \mathbf{a}_i . Although “the elementary defects” $e^{-i(\mathbf{p} \cdot \mathbf{a}_i)}$ are close to

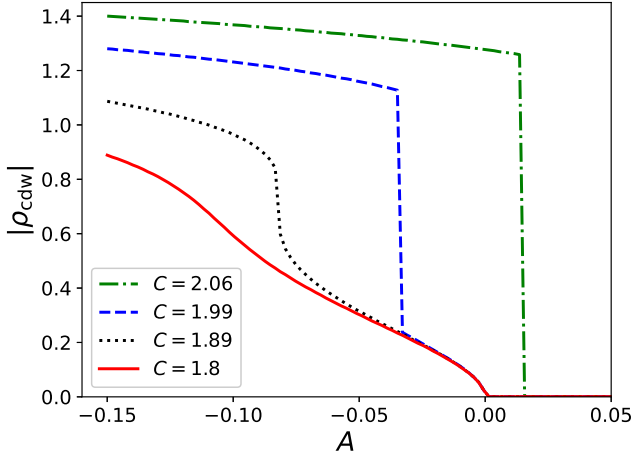


FIG. 5: Transition types in the Z_5 model, for various values of C , see legend. For larger C , the transition is first-order, as the (green) dash-dotted curve shows: when temperature grows (A increases) the order parameter $|\rho_{\text{cdw}}|$ smoothly decreases until the transition point is reached, where $|\rho_{\text{cdw}}|$ drops to zero discontinuously. When $C < 4\sqrt{2}/3$, the transition is second-order, as the solid (red) curve plotted for $C = 1.8$ demonstrates. When $4\sqrt{2}/3 < C < 5/\sqrt{6}$, the model exhibits a cascade of two transitions, see (blue) dashed curve. There is a continuous order-disorder transition at $A = 0$, and a discontinuous transition within the same CDW phase at a lower temperature. Finally, the (black) dotted curve corresponds to $C = 4\sqrt{2}/3$ (requires fine-tuning). As the system passes through ‘Cp’ point in Fig. 4 (left), a singularity $\sim \pm[1/12 + A]^{1/3}$ emerges. The influence of this singularity on the solid (red) curve is also visible.

unity, the exponent oscillates for longer translations, indicating that the contribution $\propto \rho_{\text{cdw}}^m$ averages to zero upon summation over the whole sample.

Fortunately, since $|\mathbf{p}|$ is small, the lattice can adjust its structure to allow the umklapp term. Imagine that the lattice, in response to the CDW presence, experiences an additional periodic distortion with the wave vector \mathbf{p} . Representing such a distortion by a complex quantity u , one can prove that the term $u\rho_{\text{cdw}}^m$ is invariant under the lattice translations. Indeed, a translation on \mathbf{a}_i transforms u according to the rule $u \rightarrow e^{i(\mathbf{p} \cdot \mathbf{a}_i)}u$. This makes the products $u\rho_{\text{cdw}}^m$ and $(u\rho_{\text{cdw}}^m)^*$ translation-invariant, and admissible contributions to the Landau free energy.

Conceptualizing u , one can think of it as a “frozen”, or “condensed” phonon mode, whose wave vector is \mathbf{p} . More detailed analysis of the origin of u can be found in Appendix A. There we formulate a specific model that assigns a very concrete meaning to u . In addition, we discuss a broader context within which the notion of u may be justified.

With this in mind, we write the following Landau-type

model

$$F_{\text{NC}}(\rho_{\text{cdw}}, u) = F_0(\rho_{\text{cdw}}) + \kappa_{\mathbf{p}}|u|^2 + \frac{1}{\sqrt{2m}}(g_{\text{nc}}u\rho_{\text{cdw}}^m + \text{c.c.}). \quad (34)$$

Here $\kappa_{\mathbf{p}}|u|^2 \geq 0$ is the elastic energy associated with the distortion u , complex coefficient g_{nc} is a coupling constant, and factor $(2m)^{-1/2}$ is introduced into this formula to make expression below consistent with previous definitions. (A more detailed discussion of the motivation behind Eq. (34) can be found in Appendix A.)

Minimizing this energy over u^* , we obtain

$$u = -\frac{g_{\text{nc}}^*}{\sqrt{2m}\kappa_{\mathbf{p}}}(\rho_{\text{cdw}}^*)^m. \quad (35)$$

Substituting the relation for u into Eq. (34) one derives the reduced free energy that depends on $|\rho_{\text{cdw}}|$ only

$$\tilde{F}_{\text{NC}}^{(m)} = F_0 - \frac{|c_{2m}|}{2m}|\rho_{\text{cdw}}|^{2m}, \text{ where } |c_{2m}| = \frac{|g_{\text{nc}}|^2}{\kappa_{\mathbf{p}}}. \quad (36)$$

Due to vector \mathbf{p} being small in an NC-CDW phase, the corresponding stiffness $\kappa_{\mathbf{p}}$ is small, as Appendix B demonstrates. Thus, coefficient $|c_{2m}|$ may be significant.

Note that this reduced Landau free energy is identical to $\tilde{F}^{(n)}(|\rho_{\text{cdw}}|)$ for $n = 2m$. That is, $\tilde{F}_{\text{NC}}^{(m)} \equiv \tilde{F}^{(2m)}$. Therefore, $\tilde{F}_{\text{NC}}^{(m)}$ can describe a first-order transition between the disordered and ordered phases, similar to what we have demonstrated above for Z_4 and Z_6 models. Beside this, for $m = 3$, a first-order transition within the same CDW phase, as visible in the Z_6 model phase diagram (see Fig. 4), can be realized.

In connection with the latter possibility, we would like to discuss briefly the case of EuTe_4 , see Refs. 23,24,32. There are at least two NC-CDW order parameters, one of them can be described²³ as being nearly-commensurate $\mathbf{k} \approx \mathbf{b}/m$, with $m = 3$. Inside the ordered phase a temperature-driven hysteresis loop that extends from 80 K to at least 400 K was observed. A lock-in transition behind this hysteresis was ruled out^{24,25}, since all wave vectors associated with the CDW order demonstrate remarkable thermal stability, and no commensurate diffraction peaks.

On the other hand, we can apply $\tilde{F}_{\text{NC}}^{(3)}$ to this system. Since $\tilde{F}_{\text{NC}}^{(3)}$ is identical to $\tilde{F}^{(6)}$, the two have the same phase diagram, see Fig. 4 (right). There, let us focus on the first-order transition line between ‘Cp’ and ‘T’: when this line is crossed, the amplitude $|\rho_{\text{cdw}}|$ discontinuously changes between two non-zero values. This first-order transition inside the CDW order may be the source of the hysteretic behavior of EuTe_4 .

V. DISCUSSION

We demonstrated above that the umklapp contributions to the CDW Landau free energy can qualita-

tively affect the phase diagram of a CDW-hosting material. Our approach is based on the standard McMillan-Nakanishi-Shiba framework, and represents an extension of this framework appropriate for a unidirectional commensurate or nearly-commensurate CDW.

We saw that the effects introduced by the umklapp term depend on the commensuration degree n : the larger n the richer the model's phase diagram. Indeed, for $n = 2$ the umklapp contribution does nothing but shifts the transition point, when n is as large as 5 or 6, the phase diagram displays such elements as tricritical point, critical point, continuous and discontinuous transitions lines, see Fig. 4.

Moreover, the $Z_{5,6}$ models allow for a possibility that the destruction of the order may occur through a two-step process: lower-temperature CDW-CDW discontinuous transition followed by higher-temperature CDW-disorder continuous transition, as Fig. 5 illustrates for Z_5 model. Superficially, one may argue that such a cascade was already discussed quite some time ago (see, for instance, Fig. 1 in Ref. 33, or Fig. 2 in Ref. 34). However, there is an important difference. Indeed, in our case, the first-order CDW-CDW transition occurs within the same commensurate phase. This is very much unlike commensurate-incommensurate CDW lock-in transitions of Refs. 16,33, as well as other³⁴ first-order transitions associated with discontinuous change of CDW wave vector.

We did not extend our analysis beyond $n = 6$ commensuration degree. Unfortunately, we were unable to identify any general principle restricting structure of the phase diagram of large- n models. In such a situation any investigation of a large- n case becomes problematic due to ever increasing number of parameters one must keep in the Landau free energy expansion to guarantee its stability. Yet, apart from these purely technical issues, the formulated analytical framework can be adopted to $n > 6$ models.

Our argumentation can be extended to NC-CDW order parameters as well. This is not ultimately that surprising: in a situation of small deviation from commensurability $|\mathbf{p}|$ at not-too-large n a sufficiently soft hosting crystal lattice reorganizes itself to lock-in with the CDW. This is the heuristic understanding behind Eq. (36).

This formalism can be used to explain the observed hysteretic behavior^{23,24,32} of the CDW order in EuTe_4 . The stability of the measured CDW wave vector and no commensurate diffraction peaks at any temperature are inconsistent with the lock-in CCDW/NC-CDW mechanism. On the other hand, a NC-CDW/NC-CDW transition with unchanging \mathbf{k} can be explained by the model in Sec. IV. Since the CDW in EuTe_4 is close to $m = 3$ commensuration, Eq. (36) indicates that Z_6 model may be relevant for this compound.

More “microscopic” discussion motivating the applicability of Eq. (34) to EuTe_4 and, possibly, other layered materials hosting NC-CDW can be found in Appendix A. At the same time, one must remember that the CDW

phase in EuTe_4 is quite complicated. The compound demonstrates two co-existing unidirectional order parameters with non-identical wave vectors. They interact with each other and with the lattice. Clearly, proper theoretical understanding of this complexity requires dedicated research efforts, and beyond the scope of this paper. It is also worth mentioning that Ref. 24 offers alternative explanation to the origin of the first-order transition in EuTe_4 .

We always assumed above that the system invariably chooses the global minimum of its Landau free energy. Yet for $n > 2$ our models allows for metastable states. For example, metastable minima, representing both ordered and disordered states, are clearly visible in Fig. 2, which is plotted for $n = 3$. Delayed departure from a metastable minimum reveals itself as hysteresis, a common fixture of experimental presentation of a first-order transition. Using the above phase diagrams for experimental data analysis one must remember that our calculations do not take hysteresis into account. In principle, hysteresis can be captured in the framework of the Landau theory of phase transitions. However, the description of this kind oversimplifies the physics significantly as it ignores various non-universal mechanisms affecting hysteretic behavior in real materials.

The discussed ideas can be adopted to the spin-density wave (SDW) case as well. The SDW order parameter is a complex vector \mathbf{S} , and $(\mathbf{S} \cdot \mathbf{S})$ is a true complex scalar. Thus, for even integer $n = 2k$ one can construct an umklapp term of the form $c_{2k}(\mathbf{S} \cdot \mathbf{S})^k + \text{c.c.}$ that is consistent with discrete translations, parity, and time inversion symmetries.

Finally, let us make the following observation. A number of alloys demonstrate the first-order transition between disordered and CDW phases. Several papers reporting this also commented^{10,13,14} that such an unusual transition type must be a consequence of “strong coupling”. Within the context of our formalism the expectation of strong coupling regime is quite natural: the large- n umklapp coefficients $|c_n|$ are likely to be small unless the lattice modulations associated with the order parameter are significant^{26,28}.

This suggests two things. Firstly, in order to observe the “non-trivial” features of the phase diagrams, such as the critical and tricritical points, and the first-order transition line, we should search among commensurate or nearly-commensurate CDW-hosting materials that demonstrate pronounced amplitude of the CDW modulations. A possible tool to control these amplitudes is through chemical substitution. The latter indeed can exert powerful influence on a CDW phase, as illustrated by the $R\text{Te}_3$ series whose CDW features vary dramatically as the rare-earth atom R changes³⁵.

Secondly, since in the systems of interest the order parameter amplitude must be significant, weak-coupling approximations, with their analytical or semi-analytical prescriptions for the Landau free energy coefficients, become of questionable accuracy. Thus, one must exclu-

sively employ numerical material-science methods to extract the Landau expansion. In this regard we can cite Ref. 36 which found the coefficients for a multiferroic material. Adopting this program for CCDW-hosting materials appears to be a useful direction for future research.

To conclude, in this paper, within the Landau free energy framework, we explored effects of the order parameter commensuration on the phase diagram of a CDW-hosting system. We demonstrated that in the case of commensurate and nearly-commensurate CDW the anticipated second-order transition may be replaced by the first-order transition, as indeed observed experimentally. Under certain circumstances our model predicts a cascade of two transitions (low-temperature CDW-CDW first-order transition is followed by higher-temperature order-disorder second-order transition). These ideas may be applicable to SDW phases as well.

Acknowledgments

Author is thankful to B.V. Fine, B.Q. Lv, and Alfred Zong for illuminating discussions.

Appendix A: Model of a nearly-commensurate CDW in a layered crystal

Here we describe a model in which coupling between NC-CDW and a non-CDW lattice degree of freedom give rise to the Landau energy (34). We consider a stack of \mathcal{N}_\perp weakly coupled two-dimensional (2D) units forming a quasi-2D three-dimensional body, see Fig. 6. Each unit itself is composed of two 2D lattices of non-identical chemical composition (every lattice contains \mathcal{N}_{2D} sites). One of these two lattices, denoted below as plane A, hosts a CDW instability. The other lattice (plane B) is stable by itself, but it is coupled to plane A atoms by a short-range interaction. Thus, CDW distortions, which originate in plane A, cause deformations in plane B as well.

While we do not attempt to capture the behavior of a specific material, it is worth noting that various tellurides of rare-earth elements share important similarities with such a model. For example, EuTe_4 can be viewed as a stack of flat Te planes separated by corrugated EuTe layers. The CDW is hosted by the Te layers, while EuTe planes are believed to be passive spacers²⁴.

We start formal description of our model by writing down the free energy as a sum of three terms

$$F_{\text{q2D}} = F_A + F_B + F_{AB}, \quad (\text{A1})$$

where $F_A = F_0$ describes the CDW instability inside planes A. The free energy F_B for planes B describes a stable lattice, see Appendix B. Finally, the term F_{AB}

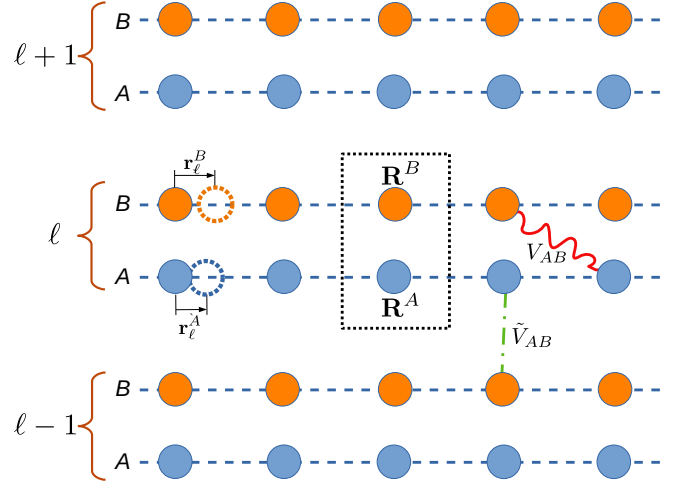


FIG. 6: Sketch of the quasi-2D crystal lattice discussed in Appendix A. The lattice is a stack of \mathcal{N}_\perp weakly coupled 2D units. Each unit itself is composed of two atomic planes, such that plane B is placed on plane A. Lattice coordinates inside the planes are denoted as $\mathbf{R}^{A,B}$. (For simplicity, the structure of 2D lattices in A and B is assumed to be the same.) Integer index $\ell = 1, \dots, \mathcal{N}_\perp$ labels the 2D units and serves as a lattice coordinate orthogonal to the planes. An elementary cell is shown as a dotted-line rectangle. It contains one atom from plane A (blue circle) and one atom from plane B (orange circle). The CDW instability is localized in planes A of each unit, while planes B experience distortions in response to the CDW. Intra-unit interaction V_{AB} is represented by (red) wavy curve, while inter-unit interaction \tilde{V}_{AB} corresponds to (green) dash-dotted line. Atoms positions distorted by the CDW are described by vectors $\mathbf{r}_\ell^{A,B}$.

represents interaction between A and B. It reads

$$F_{AB} = \sum_{\mathbf{R}^A \mathbf{R}^B \ell} V_{AB} (\mathbf{R}^A + \mathbf{r}_\ell^A - \mathbf{R}^B - \mathbf{r}_\ell^B) + \tilde{V}_{AB} (\mathbf{R}^A + \mathbf{r}_\ell^A - \mathbf{R}^B - \mathbf{r}_{\ell+1}^B). \quad (\text{A2})$$

Integer-valued index ℓ counts 2D units, while within each unit summation over every site \mathbf{R}^A in plane A and every site \mathbf{R}^B in plane B is executed. (We assume that plane A lattice is the same as plane B lattice.) Displacement of an atom from its position \mathbf{R}^A in plane A of unit ℓ is expressed by vector $\mathbf{r}_\ell^A = \mathbf{r}_\ell^A(\mathbf{R}^A)$, see Fig. 6. Similarly, displacement of an atom in plane B is expressed by vector $\mathbf{r}_\ell^B = \mathbf{r}_\ell^B(\mathbf{R}^B)$. Short-range interactions energies V_{AB} and \tilde{V}_{AB} account for intra-unit and inter-unit interactions between the atoms constituting the crystal.

Under assumption of the smallness of $|\mathbf{r}_\ell^{A,B}|$ relative to 2D lattice constant, Taylor expansion $F_{AB} = F_{AB}^0 + \delta F$ is performed, where

$$F_{AB}^0 = \mathcal{N}_\perp \mathcal{N}_{2D} \sum_{\mathbf{R}^A} V_{AB} (\mathbf{R}^A) + \tilde{V}_{AB} (\mathbf{R}^A) \quad (\text{A3})$$

is the energy of the undistorted lattice, while the correc-

tion δF due to the distortions is

$$\delta F = \sum_{\substack{\mathbf{R}^A \mathbf{R}^B \\ \ell n}} \frac{1}{n!} [(\mathbf{r}_\ell^A - \mathbf{r}_\ell^B) \cdot \nabla]^n V_{AB}(\mathbf{R}^A - \mathbf{R}^B) \quad (\text{A4})$$

$$+ \frac{1}{n!} [(\mathbf{r}_\ell^A - \mathbf{r}_{\ell+1}^B) \cdot \nabla]^n \tilde{V}_{AB}(\mathbf{R}^A - \mathbf{R}^B).$$

Here the gradient operators ∇ differentiate $V = V(\mathbf{R})$ and $\tilde{V} = \tilde{V}(\mathbf{R})$, and do not affect $\mathbf{r}_\ell^{A,B} = \mathbf{r}_\ell^{A,B}(\mathbf{R})$.

To this moment we did not assume anything specific about the distortions $\mathbf{r}_\ell^{A,B}$. Now let us imagine that the planes A distortions are associated with the CDW state

$$\mathbf{r}_\ell^A = \frac{\rho_{\text{cdw}} \mathbf{k}}{|\mathbf{k}|^2} e^{i\mathbf{k} \cdot \mathbf{R}^A} + \text{c.c.} \quad (\text{A5})$$

The distortion here is chosen to be “longitudinal”, such that $\nabla \cdot \mathbf{r}_\ell^A = i\rho_{\text{cdw}} e^{i\mathbf{k} \cdot \mathbf{R}} + \text{c.c.}$ is the (dimensionless) CDW order parameter, representing particle number per unit cell.

As planes B react passively to the CDW, displacements \mathbf{r}_ℓ^B are expected to be weaker than those in planes A: $|\mathbf{r}_\ell^B| \ll |\mathbf{r}_\ell^A|$. Due to this smallness, we will neglect those terms in δF that are second- and higher-order in $|\mathbf{r}_\ell^B|$. In this limit, we can assume simple trigonometric dependence

$$\mathbf{r}_\ell^B(\mathbf{R}^B) = \frac{u \mathbf{k}}{|\mathbf{k}|} e^{i\mathbf{p} \cdot \mathbf{R}^B} + \text{c.c.}, \quad (\text{A6})$$

where u is a complex scalar. For now, the value of the wave vector \mathbf{p} remains unconstrained. It will be determined below.

We can approximately express δF as a sum $\delta F \approx \delta F^{(0)} + \delta F^{(1)}$, where $\delta F^{(0)}$ is independent of \mathbf{r}_ℓ^B , and $\delta F^{(1)} = O(u)$. Of these two terms, $\delta F^{(0)}$ introduces renormalizations to F_A due to interaction between the CDW order parameter in planes A and undistorted lattice in planes B. We assume that all such renormalizations are already included in F_A , and will ignore $\delta F^{(0)}$.

As for $\delta F^{(1)}$, it is responsible for coupling between the CDW and plane B lattice deformation. To find $\delta F^{(1)}$, we perform two substitutions: $\mathbf{R}^A \rightarrow \mathbf{R}^A + \mathbf{R}^B$, and $n \rightarrow n + 1$. Then, introducing new notation

$$\tilde{\mathbf{r}}_\ell^A = \frac{\rho_{\text{cdw}} \mathbf{k}}{|\mathbf{k}|^2} e^{i\mathbf{k} \cdot (\mathbf{R}^A + \mathbf{R}^B)} + \text{c.c.}, \quad (\text{A7})$$

we can write

$$\delta F^{(1)} = - \sum_{\substack{\mathbf{R}^A \mathbf{R}^B \\ \ell n}} \frac{1}{n!} (\tilde{\mathbf{r}}_\ell^A \cdot \nabla)^n (\mathbf{r}_\ell^B \cdot \nabla) V_{AB}(\mathbf{R}^A) + \quad (\text{A8})$$

$$\frac{1}{n!} (\tilde{\mathbf{r}}_\ell^A \cdot \nabla)^n (\mathbf{r}_{\ell+1}^B \cdot \nabla) \tilde{V}_{AB}(\mathbf{R}^A),$$

where summation over n starts from $n = 0$, and operator ∇ acts on functions V_{AB} and \tilde{V}_{AB} only [see explanation below Eq. (A4)].

Note that lattice variable \mathbf{R}^B enters Eq. (A8) only through complex exponents of the form $e^{\pm i\mathbf{K} \cdot \mathbf{R}^B}$, where $\mathbf{K} = m\mathbf{k} \pm \mathbf{p}$, and m is a non-negative integer. In such a situation, summation over \mathbf{R}^B can be executed explicitly with the help of the “quasi-momentum conservation rule”: if \mathbf{K} belongs to the reciprocal lattice, then

$$\sum_{\mathbf{R}^B} e^{\pm i\mathbf{K} \cdot \mathbf{R}^B} = \mathcal{N}_{2D}. \quad (\text{A9})$$

Otherwise, the sum is zero.

Applying this selection rule to Eq. (A8), one finds that summation over \mathbf{R}^B produces non-zero results only when $\mathbf{p} = \mathbf{b} \pm m\mathbf{k}$, where \mathbf{b} is a reciprocal lattice vector. The terms that survive the summation are $\sim u\rho_{\text{cdw}}^m$, as well as $\sim u\rho_{\text{cdw}}^n$, $n > m$. They introduce umklapp coupling between the CDW in planes A and the lattice degrees of freedom in planes B. This derivation may be viewed as a justification for Eq. (34).

Straightforward analysis of this procedure for a generic incommensurate CDW, with small inter-plane couplings and sufficiently stiff planes B, demonstrates that the interactions between the CDW and the passive structures of the lattice introduce quantitative corrections only. Indeed, weak inter-plane coupling means that g_{nc} in definition (36) for $|c_{2m}|$ is small, while stiff planes B implies that $\kappa_{\mathbf{p}}$ in the same expression is large. These two factors act together to suppress $|c_{2m}|$, making sure that the umklapp contribution does not introduce qualitative modifications to the phase diagram.

This simple conclusion, however, must be reconsidered for an NC-CDW phase. In this case, the coupling term satisfying condition (33) is of particular importance. Since “the defect” of the NC-CDW state is small $|\mathbf{p}| \ll \pi/a$, therefore, the stiffness $\kappa_{\mathbf{p}}$, which controls the plane B distortion with the wave vector \mathbf{p} , is small as well (see Appendix B). Consequently, the coefficient $|c_{2m}|$ in Eq. (36) is large due to small denominator.

In connection with the latter observation, let us make a clarification. It appears as if $|c_{2m}|$ can become arbitrary large for very small $|\mathbf{p}|$. We must remember, however, that for very small $\kappa_{\mathbf{p}}$ the value of u in Eq. (35) becomes very large. As the whole formalism is based on u being small, the limit of very small $\kappa_{\mathbf{p}}$ should be treated by subtler approaches that account for higher-order terms u^s , $s > 1$. Also, in more sophisticated treatment, inter-layer interactions must be accounted for.

Finally, we can evaluate g_{nc} introduced in Eq. (34). The calculations below are performed for a specific case of $m = 3$, which means that $3\mathbf{k}$ is “almost” a reciprocal lattice vector. Adaptation for higher m are cumbersome but straightforward.

We start by isolating the $O(|\rho_{\text{cdw}}|^3)$ term $\delta f^{(3)}$ in Eq. (A8) and write

$$\delta f^{(3)} = -\mathcal{N}_\perp \frac{u\rho_{\text{cdw}}^3}{6|\mathbf{k}|^7} \sum_{\mathbf{R}^A \mathbf{R}^B} e^{3i\mathbf{k} \cdot (\mathbf{R}^A + \mathbf{R}^B) + i\mathbf{p} \cdot \mathbf{R}^B} (\mathbf{k} \cdot \nabla)^4 \left[V_{AB}(\mathbf{R}^A) + \tilde{V}_{AB}(\mathbf{R}^A) \right] + \text{c.c.} \quad (\text{A10})$$

Since $3\mathbf{k} + \mathbf{p}$ is a reciprocal lattice vector, summation over \mathbf{R}^B may be executed using Eq. (A9). Consequently

$$\delta f^{(3)} = -\mathcal{N}_\perp \mathcal{N}_{2D} \frac{u\rho_{\text{cdw}}^3}{6|\mathbf{k}|^7} \sum_{\mathbf{R}^A} e^{-i\mathbf{p} \cdot \mathbf{R}^A} (\mathbf{k} \cdot \nabla)^4 \left[V_{AB}(\mathbf{R}^A) + \tilde{V}_{AB}(\mathbf{R}^A) \right] + \text{c.c.} \quad (\text{A11})$$

Thus, using Eq. (34) as a definition for g_{nc} , we derive

$$g_{\text{nc}} = -\frac{\sqrt{2}}{\sqrt{3}|\mathbf{k}|^7} \sum_{\mathbf{R}^A} \cos(\mathbf{p} \cdot \mathbf{R}^A) (\mathbf{k} \cdot \nabla)^4 \left[V_{AB}(\mathbf{R}^A) + \tilde{V}_{AB}(\mathbf{R}^A) \right]. \quad (\text{A12})$$

Assume additionally that the potential energies V and \tilde{V} are short-range (that is, their characteristic space scale l_0 is smaller than the 2D lattice constant). Then the expression for g_{nc} can be simplified

$$g_{\text{nc}} \approx -\frac{\sqrt{2}\mathcal{Z}}{\sqrt{3}|\mathbf{k}|^7} \left[(\mathbf{k} \cdot \nabla)^4 (V_{AB} + \tilde{V}_{AB}) \right]_{\mathbf{R}=0}, \quad (\text{A13})$$

where \mathcal{Z} is the coordination number for a single site in the 2D lattice.

If V and \tilde{V} are characterized by an identical energy scale \tilde{V} , then Eq. (A13) can be used to write $g_{\text{nc}} \sim \mathcal{Z}\tilde{V}/(|\mathbf{k}|^3 l_0^4)$. This allows us to evaluate $|c_6| \sim \mathcal{Z}^2 \tilde{V}^2 / (|\mathbf{k}|^6 l_0^8 \kappa_{\mathbf{p}})$, where $|c_6|$ is the $m = 3$ coefficient in Eq. (36).

Let us conclude with the following observation. Our calculations in this Appendix relied on the specific model of a layered solid. While the model itself may be viewed as a very crude depiction of various layered rare-earth tellurides, we believe that the discussed theoretical framework can be extended beyond this realm. Instead of focusing of specific lattice geometry, we would like to stress the essential premise embedded into the formalism, namely the ability to split the lattice degrees of freedom into two groups: those that host the CDW instability, and those that “passively” react to the CDW formation. This grouping is quite obvious for the layered structure shown in Fig. 6, with its plane A/B dichotomy. Perhaps less clear-cut in other situations, yet it seems plausible that in a complicated multi-atomic elementary cell different atoms display different degree of participation in the CDW instability, providing an opportunity to introduce “passive distortions” of the lattice into a theoretical description. Such a reasoning can serve as a broader justification for Eq. (34).

Appendix B: Stiffness evaluation

In this Appendix we provide simple estimate for stiffness $\kappa_{\mathbf{p}}$ that first emerges in Eq. (34) and then it is

featured prominently both in Sec. IV and Appendix A. Within the model formulated in Appendix A the stiffness is a characteristics of static deformations inside plane B lattice. The corresponding potential energy is

$$F_B = \mathcal{N}_\perp \sum_{\mathbf{R}, \mathbf{R}'} V_{BB}(\mathbf{R} - \mathbf{R}' + \mathbf{r} - \mathbf{r}'), \quad (\text{B1})$$

where \mathbf{R} and \mathbf{R}' are lattice sites inside plane B. Vector $\mathbf{r} = \mathbf{r}(\mathbf{R})$, similar to $\mathbf{r}^{A,B}$ in Appendix A, represents deviation of an atom from its position \mathbf{R} . Likewise, vector $\mathbf{r}' = \mathbf{r}(\mathbf{R}')$ represents deviation of an atom from \mathbf{R}' .

For weak periodic distortion $\mathbf{r} = 2\mathbf{u} \cos(\mathbf{p} \cdot \mathbf{R} + \varphi)$, we expand F_B in powers of \mathbf{u} . Specifically, we write $F_B = F_B^{(0)} + \delta F_B$, where

$$F_B^{(0)} = \mathcal{N}_\perp \sum_{\mathbf{R}, \mathbf{R}'} V_{BB}(\mathbf{R} - \mathbf{R}') \quad (\text{B2})$$

is the energy of unperturbed lattice, and

$$\delta F_B = F_B^{(2)} + O(|\mathbf{u}|^3), \quad (\text{B3})$$

such that $F_B^{(2)} = O(|\mathbf{u}|^2)$. The first-order contribution $F_B^{(1)}$ vanishes. Indeed, one can write

$$\begin{aligned} F_B^{(1)} &= 2\mathcal{N}_\perp \sum_{\mathbf{R}, \mathbf{R}'} [\cos(\mathbf{p} \cdot \mathbf{R} + \varphi) - \cos(\mathbf{p} \cdot \mathbf{R}' + \varphi)] \times (\text{B4}) \\ &\quad (\mathbf{u} \cdot \nabla) V_{BB}(\mathbf{R} - \mathbf{R}') = \\ &\quad 2\mathcal{N}_\perp \sum_{\mathbf{R}, \mathbf{R}'} [\cos(\mathbf{p} \cdot (\mathbf{R} + \mathbf{R}') + \varphi) - \cos(\mathbf{p} \cdot \mathbf{R}' + \varphi)] \times \\ &\quad (\mathbf{u} \cdot \nabla) V_{BB}(\mathbf{R}). \end{aligned}$$

This expression vanishes due to Eq. (A9) once summation over \mathbf{R}' is performed.

To find $\kappa_{\mathbf{p}}$ we need to evaluate

$$\begin{aligned} F_B^{(2)} &= 8\mathcal{N}_\perp \sum_{\mathbf{R}, \mathbf{R}'} \sin^2(\mathbf{p} \cdot \mathbf{R}/2 + \mathbf{p} \cdot \mathbf{R}' + \varphi) \times (\text{B5}) \\ &\quad \sin^2(\mathbf{p} \cdot \mathbf{R}/2) (\mathbf{u} \cdot \nabla)^2 V_{BB}(\mathbf{R}). \end{aligned}$$

Since $\sum_{\mathbf{R}'} \sin^2(\mathbf{p} \cdot \mathbf{R}/2 + \mathbf{p} \cdot \mathbf{R}' + \varphi) = \mathcal{N}_{2D}/2$, we derive

$$F_B^{(2)} = 4\mathcal{N}_{2D}\mathcal{N}_\perp \sum_{\mathbf{R}} \sin^2(\mathbf{p} \cdot \mathbf{R}/2) (\mathbf{u} \cdot \nabla)^2 V_{BB}(\mathbf{R}). \quad (\text{B6})$$

Substituting $\mathbf{u} = |u|\mathbf{k}/|\mathbf{k}|$, in agreement with Eq. (A6), we find the desired expression for the stiffness

$$\kappa_{\mathbf{p}} = \frac{4}{|\mathbf{k}|^2} \sum_{\mathbf{R}} \sin^2(\mathbf{p} \cdot \mathbf{R}/2) (\mathbf{k} \cdot \nabla)^2 V_{BB}(\mathbf{R}). \quad (\text{B7})$$

It depends on potential energy V_{BB} , momentum \mathbf{p} , and lattice symmetry. For us it is important that for small \mathbf{p} the stiffness vanishes. Note that corrections to $\kappa_{\mathbf{p}}$ due to (weaker) inter-layer interaction were neglected in this calculation. Yet for small $\kappa_{\mathbf{p}}$ these contributions may be important.

-
- ¹ G. Grüner, *Density Waves in Solids* (Addison-Wesley, Reading, 1994).
 - ² G. Grüner, “The dynamics of charge-density waves,” *Rev. Mod. Phys.* **60**, 1129 (1988).
 - ³ A. Kogar, G. A. de la Pena, S. Lee, Y. Fang, S. X.-L. Sun, D. B. Lioi, G. Karapetrov, K. D. Finkelstein, J. P. C. Ruff, P. Abbamonte, et al., “Observation of a Charge Density Wave Incommensuration Near the Superconducting Dome in Cu_xTiSe_2 ,” *Phys. Rev. Lett.* **118**, 027002 (2017).
 - ⁴ N. Ru, C. L. Condon, G. Y. Margulis, K. Y. Shin, J. Laverock, S. B. Dugdale, M. F. Toney, and I. R. Fisher, “Effect of chemical pressure on the charge density wave transition in rare-earth tritellurides $R\text{Te}_3$,” *Phys. Rev. B* **77**, 035114 (2008).
 - ⁵ S. Pyon, K. Kudo, and M. Nohara, “Superconductivity Induced by Bond Breaking in the Triangular Lattice of IrTe_2 ,” *J. Phys. Soc. Jpn.* **81**, 053701 (2012).
 - ⁶ M. J. Eom, K. Kim, Y. J. Jo, J. J. Yang, E. S. Choi, B. I. Min, J.-H. Park, S.-W. Cheong, and J. S. Kim, “Dimerization-Induced Fermi-Surface Reconstruction in IrTe_2 ,” *Phys. Rev. Lett.* **113**, 266406 (2014).
 - ⁷ K.-T. Ko, H.-H. Lee, D.-H. Kim, J.-J. Yang, S.-W. Cheong, M. J. Eom, J. S. Kim, R. Gammag, K.-S. Kim, H.-S. Kim, et al., “Charge-ordering cascade with spin-orbit Mott dimer states in metallic iridium ditelluride,” *Nat. Commun.* **6**, 7342 (2015).
 - ⁸ K. Kim, S. Kim, K.-T. Ko, H. Lee, J.-H. Park, J. J. Yang, S.-W. Cheong, and B. I. Min, “Origin of First-Order-Type Electronic and Structural Transitions in IrTe_2 ,” *Phys. Rev. Lett.* **114**, 136401 (2015).
 - ⁹ O. Ivashko, L. Yang, D. Destraz, E. Martino, Y. Chen, C. Y. Guo, H. Q. Yuan, A. Pisoni, P. Matus, S. Pyon, et al., “Charge-Stripe Order and Superconductivity in $\text{Ir}_{1-x}\text{Pt}_x\text{Te}_2$,” *Sci. Rep.* **7**, 17157 (2017).
 - ¹⁰ B. Becker, N. G. Patil, S. Ramakrishnan, A. A. Menovsky, G. J. Nieuwenhuys, J. A. Mydosh, M. Kohgi, and K. Iwasa, “Strongly coupled charge-density wave transition in single-crystal $\text{Lu}_5\text{Ir}_4\text{Si}_{10}$,” *Phys. Rev. B* **59**, 7266 (1999).
 - ¹¹ S. Ramakrishnan, A. Schönleber, T. Rekiş, N. van Well, L. Noohinejad, S. van Smaalen, M. Tolkehn, C. Paulmann, B. Bag, A. Thamizhavel, et al., “Unusual charge density wave transition and absence of magnetic ordering in $\text{Er}_2\text{Ir}_3\text{Si}_5$,” *Phys. Rev. B* **101**, 060101 (2020).
 - ¹² Y. Singh, D. Pal, S. Ramakrishnan, A. M. Awasthi, and S. K. Malik, “Phase transitions in $\text{Lu}_2\text{Ir}_3\text{Si}_5$,” *Phys. Rev. B* **71**, 045109 (2005).
 - ¹³ Y. K. Kuo, K. M. Sivakumar, T. H. Su, and C. S. Lue, “Phase transitions in $\text{Lu}_2\text{Ir}_3\text{Si}_5$: An experimental investigation by transport measurements,” *Phys. Rev. B* **74**, 045115 (2006).
 - ¹⁴ N. S. Sangeetha, A. Thamizhavel, C. V. Tomy, S. Basu, A. M. Awasthi, P. Rajak, S. Bhattacharyya, S. Ramakrishnan, and D. Pal, “Multiple charge-density-wave transitions in single-crystalline $\text{Lu}_2\text{Ir}_3\text{Si}_5$,” *Phys. Rev. B* **91**, 205131 (2015).
 - ¹⁵ C. Young and J. Sokoloff, “The role of harmonics in the first order antiferromagnetic to paramagnetic transition in chromium,” *J. Phys. F: Met. Phys.* **4**, 1304 (1974).
 - ¹⁶ W. L. McMillan, “Landau theory of charge-density waves in transition-metal dichalcogenides,” *Phys. Rev. B* **12**, 1187 (1975).
 - ¹⁷ B. V. Fine and T. Egami, “Phase separation in the vicinity of quantum-critical doping concentration: Implications for high-temperature superconductors,” *Phys. Rev. B* **77**, 014519 (2008).
 - ¹⁸ A. Sboychakov, A. Rozhkov, K. Kugel, A. Rakhmanov, and F. Nori, “Electronic phase separation in iron pnictides,” *Phys. Rev. B* **88**, 195142 (2013).
 - ¹⁹ P. D. Grigoriev, A. A. Sinchenko, P. A. Vorobyev, A. Hadj-Azzem, P. Lejay, A. Bosak, and P. Monceau, “Interplay between band crossing and charge density wave instabilities,” *Phys. Rev. B* **100**, 081109 (2019).
 - ²⁰ V. D. Kochev, S. S. Seidov, and P. D. Grigoriev, “On the Size of Superconducting Islands on the Density-Wave Background in Organic Metals,” *Magnetochemistry* **9** (2023).
 - ²¹ S. S. Seidov, V. D. Kochev, and P. D. Grigoriev, “First-order phase transition between superconducting and charge/spin density wave states causes their coexistence in organic metals,” *Phys. Rev. B* **108**, 125123 (2023).
 - ²² M. Y. Kagan, K. Kugel, and A. Rakhmanov, “Electronic phase separation: Recent progress in the old problem,” *Phys. Rep.* **916**, 1 (2021).
 - ²³ D. Wu, Q. M. Liu, S. L. Chen, G. Y. Zhong, J. Su, L. Y. Shi, L. Tong, G. Xu, P. Gao, and N. L. Wang, “Layered semiconductor EuTe_4 with charge density wave order in square tellurium sheets,” *Phys. Rev. Mater.* **3**, 024002 (2019).
 - ²⁴ B. Q. Lv, A. Zong, D. Wu, A. V. Rozhkov, B. V. Fine, S.-D. Chen, M. Hashimoto, D.-H. Lu, M. Li, Y.-B. Huang, et al., “Unconventional Hysteretic Transition in a Charge Density Wave,” *Phys. Rev. Lett.* **128**, 036401 (2022).
 - ²⁵ B. Q. Lv, Y. Su, A. Zong, Q. Liu, D. Wu, N. F. Q. Yuan, Z. Nie, J. Li, S. Sarker, S. Meng, et al., “Large moiré superstructure of stacked incommensurate charge density waves,” (2025), arxiv:2501.09715.
 - ²⁶ Y. Feng, J. Wang, R. Jaramillo, J. van Wezel, S. Haravifard, G. Srajer, Y. Liu, Z.-A. Xu, P. B. Littlewood, and T. F. Rosenbaum, “Order parameter fluctuations at a buried quantum critical point,” *PNAS* **109**, 7224 (2012).

- ²⁷ R. Jaramillo, Y. Feng, J. Lang, Z. Islam, G. Srajer, P. Littlewood, D. McWhan, and T. Rosenbaum, “Breakdown of the Bardeen–Cooper–Schrieffer ground state at a quantum phase transition,” *Nature* **459**, 405 (2009).
- ²⁸ P. Lee, T. Rice, and P. Anderson, “Conductivity from charge or spin density waves,” *Solid State Communications* **14**, 703 (1974).
- ²⁹ K. Inagaki and S. Tanda, “Lock-in transition of charge density waves in quasi-one-dimensional conductors: Reinterpretation of McMillan’s theory,” *Phys. Rev. B* **97**, 115432 (2018).
- ³⁰ K. Inagaki and S. Tanda, “Erratum: Lock-in transition of charge density waves in quasi-one-dimensional conductors: Reinterpretation of McMillan’s theory [*Phys. Rev. B* **97**, 115432 (2018)],” *Phys. Rev. B* **99**, 249901 (2019).
- ³¹ G. L. Pascut, T. Birol, M. J. Gutmann, J. J. Yang, S.-W. Cheong, K. Haule, and V. Kiryukhin, “Series of alternating states with unpolarized and spin-polarized bands in dimerized IrTe_2 ,” *Phys. Rev. B* **90**, 195122 (2014).
- ³² Q. Q. Zhang, Y. Shi, K. Y. Zhai, W. X. Zhao, X. Du, J. S. Zhou, X. Gu, R. Z. Xu, Y. D. Li, Y. F. Guo, et al., “Thermal hysteretic behavior and negative magnetoresistance in the charge density wave material EuTe_4 ,” *Phys. Rev. B* **107**, 115141 (2023).
- ³³ W. L. McMillan, “Microscopic model of charge-density waves in $2H - \text{TaSe}_2$,” *Phys. Rev. B* **16**, 643 (1977).
- ³⁴ K. Nakanishi and H. Shiba, “Domain-like incommensurate charge-density-wave states and the first-order incommensurate-commensurate transitions in layered tantalum dichalcogenides. I. 1T-polytype,” *J. Phys. Soc. Jpn.* **43**, 1839 (1977).
- ³⁵ B. F. Hu, B. Cheng, R. H. Yuan, T. Dong, and N. L. Wang, “Coexistence and competition of multiple charge-density-wave orders in rare-earth tritellurides,” *Phys. Rev. B* **90**, 085105 (2014).
- ³⁶ S. Artyukhin, K. T. Delaney, N. A. Spaldin, and M. Mostovoy, “Landau theory of topological defects in multiferroic hexagonal manganites,” *Nat. Mater.* **13**, 42 (2014).